

# A novel hybrid surface micromachined segmented mirror for large aperture laser applications

Jie Li (李捷), Haiqing Chen (陈海清), and Hongbin Yu (余洪斌)

Department of Opto-Electronics Engineering, Huazhong University of Science and Technology, Wuhan 430074

Received October 27, 2005

A novel hybrid surface micromachined segmented mirror array is described. This device is capable of scaling to large apertures for correcting time-varying aberrations in laser applications. Each mirror is composed of bottom electrode, support part, and mirror plate, in which a T-shaped beam structure is used to support the mirror plate. It can provide mirror with vertical movement and rotation around two horizontal axes. The test results show that the maximum deflection along the vertical direction of the mirror plate is  $2\ \mu\text{m}$ , while the rotation angles around  $x$  and  $y$  axes are  $\pm 2.3^\circ$  and  $\pm 1.45^\circ$ , respectively.

OCIS codes: 230.0230, 140.0140, 310.0310, 040.6040.

Many high power lasers typically suffer from reduced beam quality due to thermally induced aberrations. A deformable mirror in combination with a wave-front sensor and a real-time controller can be used to correct time-varying aberrations in laser applications. Most deformable mirrors that are commercially available today are macroscopic devices made with flat glass mirror plates supported by an array of piezoelectric actuators. Deformable mirrors based on micro-electro-mechanical system (MEMS) technology hold the promise of an inexpensive low-power and high performance alternative to existing designs.

A variety of MEMS-based deformable mirrors have been investigated<sup>[1-5]</sup>. Figure 1 shows some of these mirror systems. Continuous membrane mirrors<sup>[1-3]</sup> (Fig. 1(a)) have the advantage that they cause almost no diffraction of the reflected beam and ensure continuous phase variations across the mirror. Unfortunately the majority of the mirrors using this technology do not scale to large apertures, and the inter-actuator coupling is high. Segmented mirrors<sup>[4]</sup> (Fig. 1(b)), capable of pure piston motion only, exhibit no inter-actuator coupling but may produce undesirable diffraction due to the gaps between adjacent segments. Hybrid mirror designs<sup>[5]</sup> that permit tip-tilt motion in addition to piston motion (Fig. 1(c)) allow optical phase to be matched at the interface between adjacent mirror segments. This feature ensures phase continuity across the entire mirror face. A MEMS-based two-axis optical scanner array with a high factor and large mechanical scan angles was reported by Tsai *et al.*<sup>[5]</sup>.

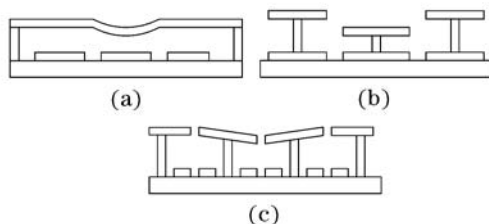


Fig. 1. Schematic of deformable mirror array sections with (a) continuous mirrors, (b) segmented mirrors with piston motion, and (c) segmented mirrors having tip-tilt motion.

In this paper, we propose a novel hybrid micromirror structure, in which two T-shaped beams placed symmetrically are used to support mirror plate, thus enabling mirror to move vertically and rotate around two horizontal axes.

The designed micromirror is composed of a mirror plate, four mirror support posts, two T-shaped beams, a beam support post, and bottom electrodes. The upside of mirror plate is used to reflect the incident light and is coated with a thin layer of Au for the reflectivity improvement, while the backside acts as the upper electrode and is connected to beams through four posts. Figure 2 shows the schematic of the designed mirror, and the specific T-shaped beam is shown in Fig. 3.

The prominent advantage of this type of micromirror is its ability to be actuated with three modes: piston mode along  $z$ -axis, tilt modes around  $x$  and  $y$  axes. When a voltage is applied to all the four bottom electrodes, the mirror plate will deflect toward substrate by the electrostatic force. When a voltage is only applied to any two

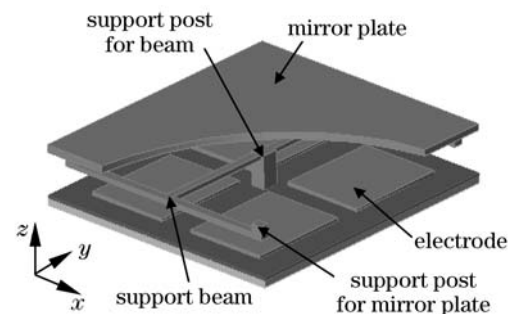


Fig. 2. Schematic of the designed micromirror.

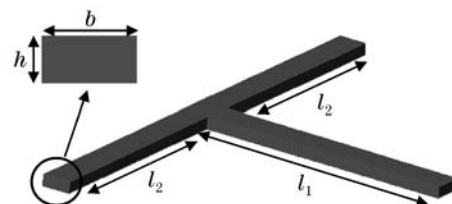


Fig. 3. Schematic of the T-shaped beam.

electrodes placed along  $x$ - or  $y$ -axis, the mirror plate will rotate around corresponding axis and be tilted toward the electrodes. In the case of piston mode, the mirror plate is landed on the support post for beam, while in the case of tilt mode, the tip of the beam is landed on the insulated region of substrate, thus preventing an electrical shot between electrodes. The static characteristics are analyzed below for all of the movements.

In the case of piston mode operation, the spring constant  $k'$  of the T-shaped beam can be calculated by

$$k' = \frac{Ebh^3}{2l_1^3 + l_2^3}, \quad (1)$$

where  $E$  is the Young's modulus,  $b$  is the beam width,  $h$  is beam thickness,  $l_i$  ( $i = 1, 2$ ) is the length of each section.

In the case of two tilt modes operation, when a unit torque is applied to mirror plate, the deflection angle around  $x$  and  $y$  axes can be given by

$$\phi_x = \frac{Ebh^3}{2l_1 + \frac{l_2^3}{l_1^2}}, \quad \phi_y = \frac{bh^3}{\frac{l_2}{E} + \frac{l_1}{2\beta G}}, \quad (2)$$

where  $G$  is the shear modulus,  $\beta$  is torsional factor according to the ratio between beam width and thickness. With the designed beam dimensions described in Table 1 and with  $E$  and  $G$  of phosphorus-doped polysilicon ( $E = 155$  GPa and  $G = 64$  GPa), we can get:  $k' = 2.363$  N/m,  $\phi_x = 0.449 \times 10^{-10}$  N·m/rad, and  $\phi_y = 0.314 \times 10^{-10}$  N·m/rad.

From the results, it is obvious that the rotation around  $y$ -axis is much easier than that around  $x$ -axis.

The micromirror was fabricated using standard surface micromachining technology. Six masks were required in

**Table 1. Dimensions of Designed Structure (Unit:  $\mu\text{m}$ )**

Part	Size
Mirror Plate	$80 \times 80 \times 2$
Supporting Beam	$l_1$ 33
	$l_2$ 39
	$b$ 2
	$h$ 1
Spacing between Mirror and Beam	2
Spacing between Beam and Bottom Electrode	3

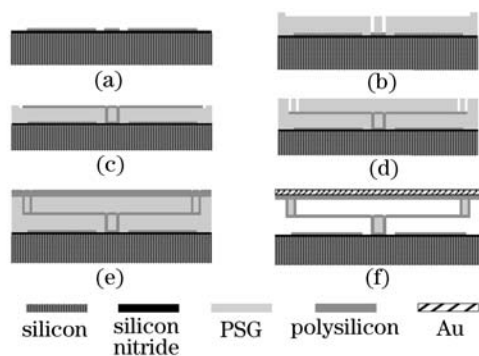


Fig. 4. Fabrication process.

the fabrication process. Polysilicon was selected as the structural material and phospho-silicate glass (PSG) was used as sacrificial layer. Figure 4 shows the fabrication process and the fabricated micromirror array is shown in Fig. 5.

Figure 6 shows the deflection in  $z$  direction as a function of the voltage applied to all of the bottom electrodes. The measured maximum deflection was  $2 \mu\text{m}$  at  $78$  V. Above this critical point, further increasing the voltage cannot influence the deflection due to the contact between mirror plate and post. In the case of tilt measurement, the maximum deflection angles were measured as  $1.45^\circ$  at  $92$  V and  $2.3^\circ$  at  $63$  V, respectively, for rotation around  $x$  and  $y$  axes, as shown in Fig. 7. From the structure, we can see that all of the three motions are limited by the thickness of corresponding sacrificial layers, as a result, a larger deflection can be expected by using thicker sacrificial layer.

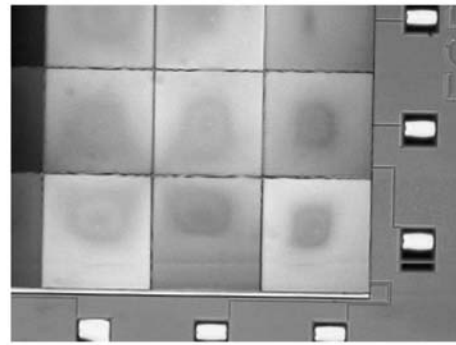


Fig. 5. SEM photograph of the fabricated mirror.

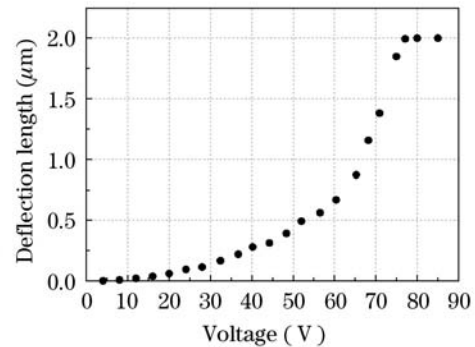


Fig. 6. Measured deflection length as a function of applied voltage.

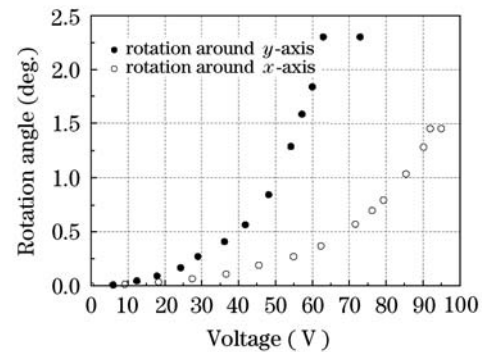


Fig. 7. Rotation angle as a function of applied voltage.

In summary, a  $3 \times 3$  micromirror array was designed and successfully fabricated using surface micromachining technology. The mirror plate was suspended over the substrate through two T-shaped beams, with which it had the potential use in the application of phase and amplitude modulation for large aperture lasers. The test results show that the maximum deflection along the vertical direction of the mirror plate is  $2 \mu\text{m}$ , corresponding to  $12\pi$  phase modulation for 633-nm He-Ne laser, while the rotation angles around  $x$  and  $y$  axes are  $\pm 2.3^\circ$  and  $\pm 1.45^\circ$ , respectively.

This work was supported by the National Natural Science Foundation of China under Grant No. 10476010. J. Li's e-mail address is lj14163@yahoo.com.cn.

## References

1. J. D. Mansell, S. Sinha, and R. L. Byer, Proc. SPIE **4493**, 1 (2002).
2. G. Vdovin and P. M. Sarro, Appl. Opt. **34**, 2968 (1995).
3. L. M. Miller, M. L. Agronin, R. K. Bartman, W. J. Kaiser, T. W. Kenny, R. L. Norton, and E. C. Vote, Proc. SPIE **1945**, 421 (1993).
4. M. C. Roggeman, V. M. Bright, B. M. Welsh, S. R. Hick, P. C. Roberts, W. D. Cowan, and J. H. Comtois, Opt. Eng. **36**, 1326 (1997).
5. J.-C. Tsai and M. C. Wu, Journal of Microelectromechanical System **14**, 1323 (2005).